ARTICLE

Colorimetric Detection of Pb^{2+} Using Glutathione Functionalized Gold Nanoparticles

Fang Chai,[†,‡] Chungang Wang,[†] Tingting Wang,[†] Lu Li,[†] and Zhongmin Su*[,†]

Institute of Functional Material Chemistry, Faculty of Chemistry, Northeast Normal University, Changchun, 130024, P.R. China, and College of Chemistry & Chemical Engineering, Harbin Normal University, Harbin, 150025, P. R. China

ABSTRACT A facile, cost-effective and sensitive colorimetric detection method for Pb^{2+} has been developed by using glutathione functionalized gold nanoparticles (GSH-GNPs). The sensitivity and selectivity of detection were investigated in detail. The GSH-GNPs could be induced to aggregate immediately in the presence of Pb^{2+}, especially after the addition of 1 M NaCl aqueous solution. The Pb^{2+} could be detected by colorimetric response of GNPs that could be monitored by a UV−vis spectrophotometer or even naked eyes, and the detection limit could reach 100 nM. The GSH-GNPs bound by Pb^{2+} showed excellent selectivity compared to other metal ions (Hg^{2+}, Mg^{2+}, Zn^{2+}, Ni^{2+}, Cu^{2+}, Co^{2+}, Ca^{2+}, Mn^{2+}, Fe^{2+}, Cd^{2+}, Ba^{2+}, and Cr^{3+}), which led to prominent color change. This provided a simple and effective colorimetric sensor (no enzyme or DNA) for on-site and real-time detection of Pb^{2+}. Most importantly, this probe was also applied to determine the Pb^{2+} in the lake samples with low interference and high sensitivity.

KEYWORDS: lead(II) ion • glutathione • gold nanoparticle • colorimetry • detection

INTRODUCTION

Gold nanoparticles (GNPs) are widely used in a range of applications, including electronics, biosensing, and surface enhanced Raman spectroscopy. GNPs have also received great attention in the development of visual sensing schemes owing to the surface plasmon resonance (SPR) mechanism based on the binding-induced aggregation of spherical GNPs (1−3). The SPR of the GNPs are extremely sensitive to their nature, size, shape, their interparticle distances, and the nature of their surrounding media (4). Recently, GNPs have been extensively employed as analytical probes in biotechnological and chemical systems. In particular, Mirkin and co-workers demonstrated that the distance-dependent SPR property of GNPs aggregation induced by DNA hybridization was exploited for developing a colorimetric sensor for DNA, Hg^{2+} detection (5, 6). Furthermore, functionalized GNPs become interesting nanomaterials for sensing heavy metal ions (7, 8).

The contamination by heavy metal ions, particularly Pb^{2+}, poses a serious threat to human health and environment. Lead-poisoning causes renal malfunction and inhibits brain development associated with environmental pollution, particularly in children, causing various neurotoxic effects (9). As lead is nondegradable, it is persistent in the environment and can produce toxic effects in plants and animals (10). Traditional methods such as inductively coupled plasma mass spectrometry often require expensive and sophisticated instrumentation and complicated sample preparation processes (10).

On the basis of the aforementioned facts, it is critical to develop probes that provide rapid on-site evaluation of Pb^{2+}. Toward this goal, a variety of methods have been developed by means of GNPs, fluorophores, DNAzymes, and polymers (11−14). Among them, colorimetric sensors offer a promising approach for facile tracking of metal ions in biological, toxicological, and environmental samples. Lu and co-workers have developed a series of functional DNAzyme-based sensors by using GNPs. The detection range of the sensor could be tuned from 3 nM to 1 μM (15−19). Dong and co-workers reported a DNAzyme-based colorimetric sensor for Pb^{2+}, the detection limit was 500 nM (20). These studies demonstrated high sensitivity and selectivity. In spite of good selectivity, these methods require a procedure with complex labeling or surface functionalization chemistry. The synthesis of DNA oligomers and their chemical modification with GNPs were complex and expensive. Additionally, the stability of DNA probes limited their applications for many real samples. Recently, Ying et al. have reported GSH-capped ZnCdSe and CdTe QDs as selective fluorescent Pb^{2+} probes with low detection limit (20 nM) (21). And glutathione (GSH, γ-Glu-Cys-Gly) played a crucial role in protecting intracellular components against oxidative damage and detoxifying heavy metal ions through the mercapto group in an organism (22). In particular, GSH has two free −COOH groups and a NH_2 group to provide a hydrophilic interface and a handle for further reactivity with other functional molecules. In this study, we present a simple, sensitive, and selective colorimetric probe for the detection of Pb^{2+}-based on GSH-GNPs.

* To whom correspondence should be addressed. E-mail: zmsu@nenu.edu.cn.
Received for review February 5, 2010 and accepted April 21, 2010
† Northeast Normal University.
‡ Harbin Normal University.
DOI: 10.1021/am100107k

Published on Web 04/29/2010

To demonstrate the practicality of the present approach, this probe was applied to determine the Pb^{2+} in the lake samples.

EXPERIMENTAL SECTION

Chemicals and Materials. All chemicals used were of analytical grade or of the highest purity available. Chloroauric acid ($HAuCl_4 \cdot 3H_2O$) and sodium borohydride ($NaBH_4$ 98%) were obtained from Sigma Aldrich (USA) and used as received. Glutathione were purchased from Genview. The used metal salts $Pb(NO_3)_2$, $Ni(NO_3)_2 \cdot 6H_2O$, $Cd(NO_3) \cdot 4H_2O$, $FeCl_2 \cdot 4H_2O$, $Mg(NO_3)_2 \cdot 6H_2O$, $CaCl_2 \cdot 2H_2O$, $Co(Ac)_2 \cdot 6H_2O$, $Zn(Ac)_2 \cdot 2H_2O$, $BaCl_2 \cdot 2H_2O$, $CuSO_4 \cdot 5H_2O$, $Hg(NO_3)_2 \cdot 2H_2O$, and NaCl were purchased from Beijing Chemical Reagent Company (Beijing, China). The Pb^{2+} stock solution was 5 mM. All glassware was thoroughly cleaned with freshly prepared aqua regia (3:1 (v/v) HCl/HNO_3 and rinsed thoroughly with Mill-Q (18 MΩ cm^{-1} resistance) water prior to use. Mill-Q water was used to prepare all the solutions in this study.

Methods. The morphology and size of the GSH-GNPs were characterized by transmission electron microscopy (TEM) using a JEOLFETEM-2100 transmission electron microscope operated at an accelerating voltage of 200 kV. Absorption spectra were recorded on a UV−vis spectroscopy performed with a U-3010 spectrophotometer (Hitachi, Japan) at room temperature.

Preparation of GNPs Coated with GSH. The preparation of GSH-GNPs was synthesized according to the procedure described previously with a slightly modification (23). Briefly, An aqueous solution of tetrachloroauric acid ($HAuCl_4 \cdot 3H_2O$, 1 mL, 0.025 M) was mixed with an aqueous solution of GSH (7.8 mL, 0.019 M). The pH of the resulting mixture was adjusted to 8.0 using 1 M NaOH. A freshly prepared $NaBH_4$ solution (2 mg/mL in water, 10-fold molar excess) was added with stirring. The mixture was allowed to react overnight at room temperature. The free GSH molecules in solution were removed by centrifugation at 6000 rpm for 10 min, then the GSH-GNPs were obtained.

Colorimetric Detection of Pb^{2+}. The as-prepared GSH-GNPs were diluted to four times by water, and the resulting concentration was about 51.2 nM calculated according to the previous literature (24). $Pb(NO_3)_2$ stock solution was used for the Pb^{2+} sensitivity studies. Various concentrations of Pb^{2+} were prepared using serial dilution of the stock solution to test the sensitivity limits of the GSH-GNPs. Using the stock solution, 0.05−50.0 μM of Pb^{2+} were prepared. The colorimetric detection of aqueous Pb^{2+} was performed at room temperature. Briefly, 100 μL of GSH-GNPs solution was added 120 μL of Pb^{2+} with different concentrations. The GSH-GNPs turned purple as they met Pb^{2+} at high ionic strength, indicating formation of aggregates (25, 26). The addition of enough salt could screen the repulsion between the negatively charged GNPs, leading to the aggregation of the GNPs followed by a corresponding color change, so we tested the addition of 20 μL 1 M NaCl into GSH-GNPs, resulting in a color change quickly. In the experiments of selectivity and practical assay, all samples were tested in a similar way. We investigated the selectivity of our new approach for Pb^{2+} over other metal ions (Cd^{2+}, Cr^{3+}, Ba^{2+}, Zn^{2+}, Ca^{2+}, Mn^{2+}, Mg^{2+}, Fe^{2+}, Co^{2+}, Ni^{2+}, Cu^{2+}, Hg^{2+}) under the same conditions.

RESULTS AND DISCUSSION

Mechanistic Basis for the Sensing System. GSH-GNPs were used as probes for detecting Pb^{2+}. The as-prepared GSH-GNPs are stable because the GSH protects the GNPs from aggregation in the presence of a given high concentration of salt. GSH has two free −COOH groups and a $-NH_2$ group to provide a hydrophilic interface and a

Scheme 1. Strategy for the Colorimetric Detection of Pb^{2+} Using GSH-GNPs

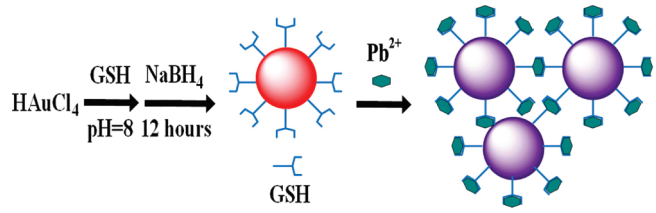

handle for further reactivity with heavy metal ions. GSH can capture Pb^{2+} in aqueous solution resulting in the aggregation of GNPs. As shown in scheme 1, aggregation of GSH-GNPs in the presence of Pb^{2+} is due to the binding with chelating ligands, yielding both a substantial shift in the plasmon band energy to longer wavelength and a red-to-blue color change.

Colorimetric Detection of Pb^{2+}. GSH-GNPs were characterized by UV−vis spectroscopy and TEM. As shown in Figure 1, a characteristic SPR band of GSH-GNPs was observed in the spectrum at approximate 520 nm (Figure 1A, curve a) and the color of the solution remained red (Figure 1A, inset a) in the absence of Pb^{2+}. The corresponding TEM image was shown in Figure 1B(a) and the as-prepared GSH-GNPs were dispersed with about 5−8 nm in diameter (23). Upon addition of 10 μM Pb^{2+} to GSH-GNPs, the solution turned purple owing to the Pb^{2+}-stimulated aggregation, further supported by TEM image (Figure 1B(b)) (27, 28), along with broadening and shifting of the SPR peak.

To evaluate the detectable minimum concentration of Pb^{2+} in aqueous solution by color change, we added the Pb^{2+} with concentrations of 5−50 μM into GSH-GNPs solution. From Figure 3, when the concentration of Pb^{2+} increased from 0.1 to 50 μM, a red shift in wavelength and a broadening of the SPR occurred. The color changed from red to violet accompanied with a bathochromic shift, indicating a clear detection result as shown in Figure S1 (see the Supporting Information). The change of SPR band is attributed to the

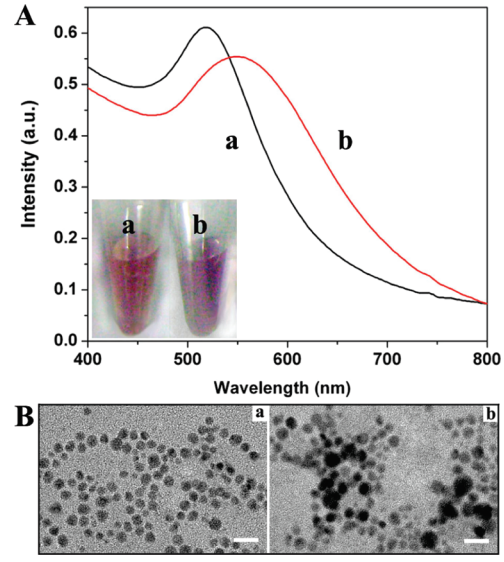

FIGURE 1. (A) UV−vis spectra and (B) TEM images of the GSH-GNPs in the (a) absence and (b) presence of 10 μM Pb^{2+} solution; inset image is colorimetric response (scale bars: 10 nm).

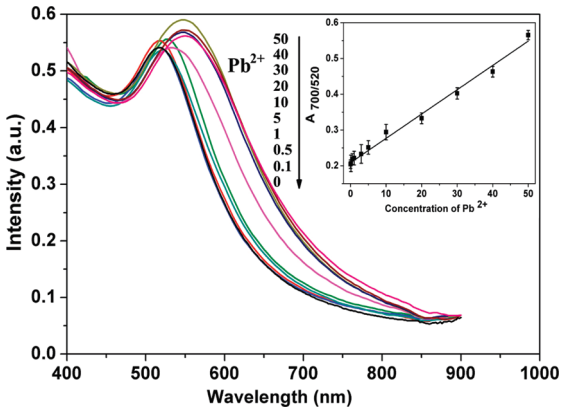

FIGURE 2. UV−vis absorption spectra of GSH-GNPs after the addition of different concentrations of Pb^{2+} (0, 0.1, 0.5, 1, 5, 10, 20, 30, 40, 50 μM). The inset shows a plot of $A_{700/520}$ versus the concentrations of Pb^{2+} in the range of 0.1−50 μM. The error bars represent standard deviations based on three independent measurements.

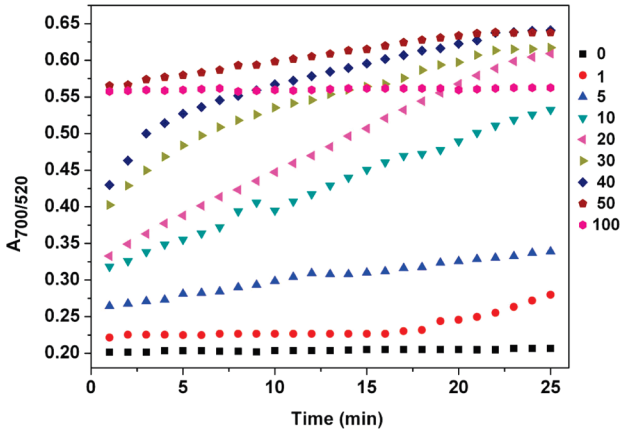

FIGURE 3. Plots of the time-dependent absorption ratio ($A_{700/520}$) over 25 min (100 μL of GSH-GNPs solution in the presence of various concentrations of Pb^{2+} after the addition of 20 μL of 1 M NaCl).

coupled plasmon absorbance of nanoparticles in close contact. The SPR of the GSH-GNPs solution at 700 and 520 nm are related to the quantities of dispersed and aggregated GSH-GNPs, respectively. Thus, we used the ratio of the values of Absorbance 700/520 ($A_{700/520}$) to express the molar ratio of aggregated and dispersed GSH-GNPs.A linear relationship between $A_{700/520}$ and the Pb^{2+} concentration was observed from 0.1 to 50 μM (R^2 = 0.9912) (inset of Figure 2). Therefore, we suggest that this probe can be used for detecting Pb^{2+} with a minimum detectable concentration of 100 nM.

The response of the GSH-GNPs was obtained at various reaction time (Figure 3). The results showed that the absorption ratio ($A_{700/520}$) increased with the binding time. The $A_{700/520}$ values of GSH-GNPs upon the addition of 30, 40, 50, 100 μM Pb^{2+} reached a maximum at about 20−25 min, whereas the values of the addition of other concentrations (5−20 μM) of Pb^{2+} kept increasing. When the GSH-GNPs met 100 μM of Pb^{2+}, the response completed immediately, indicating that the aggregation response of GSH-GNPs was highly dependent on the concentration of Pb^{2+}. The aggregation of GSH-GNPs induced by a high concentration of Pb^{2+} resulted in a decrease in the intensity of absorption due to the precipitation in solution (see Figure S2 in the Supporting Information). This result represents the fast performance of this probe for Pb^{2+}.

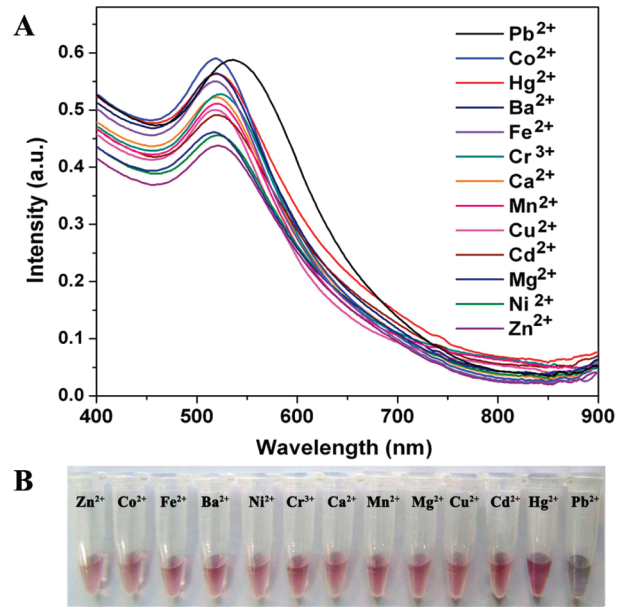

FIGURE 4. (A) UV−vis absorption spectra and (B) the corresponding photo images of GSH-GNPs containing 50 μM other metal ions compared with 20 μM Pb^{2+} (metal ions were incubated with GSH-GNPs for 20 min).

Selectivity Test. Several commonly existing metal ions were tested including Zn^{2+}, Co^{2+}, Fe^{2+}, Ba^{2+}, Ni^{2+}, Cr^{3+}, Ca^{2+}, Mn^{2+}, Mg^{2+}, Cu^{2+}, Hg^{2+}, and Cd^{2+} ions. The SPR band and the corresponding photo images of GSH-GNPs containing 50 μM other metal ions and 20 μM Pb^{2+} were shown in Figure 4. The results demonstrate 50 μM Zn^{2+}, Co^{2+}, Fe^{2+}, Ba^{2+}, Ni^{2+}, Cr^{3+}, Ca^{2+}, Mn^{2+}, Mg^{2+}, Cu^{2+}, Cd^{2+}, and Hg^{2+} have no obvious effect on the SPR band and color of GSH-GNPs as compared to 20 μM Pb^{2+}, which made the color of solution change from red to blue gray under otherwise the same conditions, indicating that the assay approach has very high specificity toward Pb^{2+}.

We also investigated the changes in values of absorption ratio ($A_{700/520}$) for GSH-GNPs that occurred after 20 min upon the addition of the metal ions (Zn^{2+}, Co^{2+}, Fe^{2+}, Ba^{2+}, Ni^{2+}, Cr^{3+}, Ca^{2+}, Mn^{2+}, Mg^{2+}, Cu^{2+}, Hg^{2+} and Cd^{2+}) at the same conditions (Figure 5). Only Pb^{2+} sample showed a significant value at all concentrations. Additionally, 100 and 250 μM of each metal ion added into GSH-GNPs as control experiments were performed. As shown in Figure S3 in the Supporting Information, values of absorption ratio ($A_{700/520}$) of GSH-GNPs upon the addition of each ion increased with the increase of concentration. But the values ($A_{700/520}$) exceeded to 0.3 when the concentrations of Hg^{2+} and Mn^{2+} were higher than 50 μM, and the color of GSH-GNPs turned purple. Apparently, 1 mM Co^{2+} and Zn^{2+} and 500 μM Fe^{2+} and Ca^{2+} could not induce the color change of the GSH-GNPs. On the basis of the aforementioned results, we concluded that GSH-GNPs can be utilized to detect Pb^{2+} with high sensitivity and selectivity. The mechanism can be attributed to the function of Pb^{2+} with GSH in a chelating reaction. The aggregation of GSH-GNPs was induced by the coordination

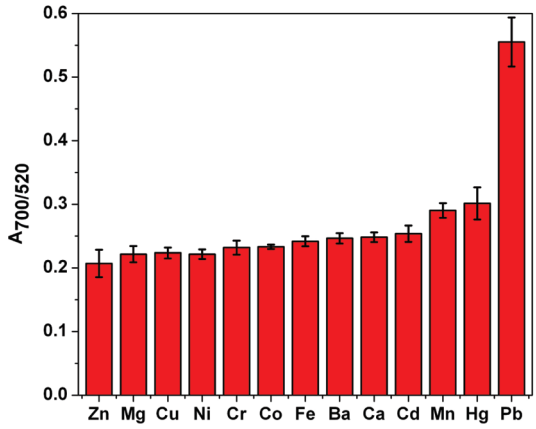

FIGURE 5. The values ($A_{700/520}$) of GSH-GNPs upon the addition of 50 μM ions. The error bars represent standard deviations based on three independent measurements.

between Pb^{2+} and carboxylate of GSH (21). However, it would be difficult to rationalize the selective response toward Pb^{2+}.

To further evaluate the mechanism, we monitored the aggregation kinetics of GSH-GNPs after addition of 50 μM of ions (see Figure S4 in the Supporting Information). Plots of the time-dependent absorption ratio ($A_{700/520}$) over 40 min of GSH-GNPs with 50 μM ions were obtained. All values of $A_{700/520}$ were increased with the time of ions reacting with GSH-GNPs, and in all cases, the Pb^{2+} exhibited a stronger signal than that of any of the other metal ions. It might be nominated that the color changes of GSH-AuNPs upon the addition of 50 μM Mn^{2+}, Hg^{2+}, and Cd^{2+} need about 40−100 min at the same conditions, whereas GSH-GNPs samples upon the addition of Ba^{2+}, Co^{2+}, Mg^{2+}, Zn^{2+}, Cu^{2+}, Ni^{2+}, Ca^{2+}, and Fe^{2+} have no color change in 2 days. We believe that the explanation of selectivity is probably because the aggregation rates of other ions were relatively slow as compared to Pb^{2+}. The detailed mechanism of selectivity still needs further investigation.

Practical Application. In certain environmental samples, such as lake water, the concentrations of some metal ions or some unknown contamination are significantly higher than that of Pb^{2+}, so potential practical assay is necessary, and it is a critical issue to the application of most common sensors. To confirm the practical application of the probes, we collected water samples from a freshwater lake in our campus and filtered through a 0.2 μm membrane then analyzed by ICP-MS (see Table S1 in the Supporting Information). Pb^{2+} ions were not detected in the lake water samples, in good agreement with ICP-MS data. We then prepared a series of samples by spiking them with standard solution (29−33) of Pb^{2+} over the range 0.1−50 μM. The detection results of Pb^{2+} in lake water samples were shown in Figure 6, indicating this method is largely free from the matrix effect of the lake water sample. There is a good linear relationship between the $A_{700/520}$ with different concentrations of Pb^{2+}(0.1−10 μM) with $R^2 = 0.9851$. The lowest detectable concentration of Pb^{2+} in the lake water was also 100 nM.

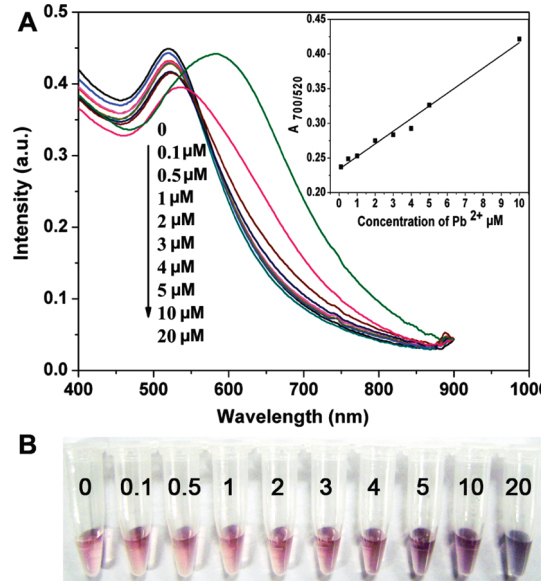

FIGURE 6. (A) UV−vis absorption spectra of samples of lake water and (B) the corresponding photo images of the concentrations of Pb^{2+} in lake water ranging from 0, 0.1, 0.5, 1, 2, 3, 4, 5, 10, to 20 μM from left to right. The inset shows a plot of $A_{700/520}$ versus the concentrations of Pb^{2+} in the range of 0.1−10 μM.

To further evaluate the selectivity (21), the Pb^{2+} detection in the presence of other metal ions was also investigated. The mixture solution was prepared with 10 μL each of 100 μM concentrations of 12 kinds of ions in lake water (Zn^{2+}, Co^{2+}, Fe^{2+}, Ba^{2+}, Ni^{2+}, Cr^{3+}, Ca^{2+}, Mn^{2+}, Mg^{2+}, Cu^{2+}, Hg^{2+}, and Cd^{2+}); 20, 10, 5, 2, 1, 0.5, 0.2 and 0.1 μM Pb^{2+} solutions were diluted by equivalent mixture solutions containing 12 kinds of ions. The as-prepared 10, 5, 2.5, 1, 0.5, 0.25, 0.1, and 0.05 μM mixture solutions containing Pb^{2+} were then added into GSH-GNPs in the presence of 20 μL of 1 M NaCl. The results indicated good adaptability of GSH-GNPs, which can be observed from the Supporting Information (Figures S5−S8). However, the mixture solution was prepared by 10 μL each of 500 μM concentrations of other ions, the detection of Pb^{2+} by GSH-GNPs was interfered because the GSH-GNPs occurred a similar aggregation in the presence of Hg^{2+}, Mn^{2+}, and Cd^{2+}.

CONCLUSIONS

In summary, a simple, cost-effective, portable detection method using GSH-GNPs-based colorimetric probe that allows rapid, on-site, real-time detection of Pb^{2+} has been developed. The experimental results show that Pb^{2+} can be detected quickly and accurately with high sensitivity and selectivity against other heavy metal ions. We believed this method may offer a new approach for the detection of Pb^{2+} in aqueous biological and environmental samples.

Acknowledgment. The authors gratefully acknowledge the financial support from the National High-tech Research and Development Program of China (863 Program 2007AA03Z354), the National Natural Science Foundation of China (Project 20703009, 20971020), Program for Changjiang Scholars and Innovative Research Team in University (IRT0714), and Department of Science and Technology of Jilin Province (20082103).

Supporting Information Available: Photo images and UV−vis spectra of Pb^{2+} detection by GSH-GNP probes (PDF). This material is available free of charge via the Internet at http://pubs.acs.org.

REFERENCES AND NOTES

(1) El-Sayed, M. A. *Acc. Chem. Res.* **2001**, *34*, 257–264.
(2) Hutter, E.; Pileni, M.-P. *J. Phys.Chem. B* **2003**, *107*, 6497–6499.
(3) Tokareva, I.; Minko, S.; Fendler, J. H.; Hutter, E. *J. Am. Chem. Soc.* **2004**, *126*, 15950–15951.
(4) Liu, C. W.; Huang, C. C.; Chang, H. T. *Langmuir* **2008**, *24*, 8346–8350.
(5) Mirkin, C. A.; Letsinger, R. L.; Mucic, R. C.; Storhoff, J. J. *Nature* **1996**, *382*, 607–609.
(6) Lee, J. S.; Han, M. S.; Mirkin, C. A. *Angew. Chem., Int. Ed.* **2007**, *46*, 4093–4096.
(7) Liu, J.; Cao, Z.; Lu, Y. *Chem. Rev.* **2009**, *109*, 1948–1998.
(8) Chai, F.; Wang, C. G.; Wang, T. T.; Ma, Z. F.; Su, Z. M. *Nanotechnology* **2010**, *21*, 025501.
(9) Shen, L.; Chen, Z.; Li, Y. H.; He, S. L.; Xie, S. B.; Xu, X. D.; Liang, Z. W.; Meng, X.; Li, Q.; Zhu, Z. W.; Li, M. X.; Le, X. C.; Shao, Y. H. *Anal. Chem.* **2008**, *80*, 6323–6328.
(10) Li, Y.; Chen, C.; Li, B.; Sun, J.; Wang, J.; Gao, Y.; Zhao, Y.; Chai, Z. *J. Anal. At. Spectrom.* **2006**, *21*, 94–96.
(11) Zuo, P.; Yin, B. C.; Ye, B. C. *Biosens. Bioelectron.* **2009**, *25*, 935–939.
(12) Slocik, J. M.; Zabinski, J. S.; Phillips, D. M.; Naik, R. R. *Small* **2008**, *4*, 548–551.
(13) Si, S.; Raula, M.; Paira, T. K.; Mandal, T. K. *Chem. Phys. Chem.* **2008**, *9*, 1578–1584.
(14) Li, T.; Wang, E. K.; Dong, S. J. *J. Am. Chem. Soc.* **2009**, *131*, 15082–15083.
(15) Liu, J. W.; Lu, Y. *J. Am. Chem. Soc.* **2003**, *125*, 6642–6643.
(16) Liu, J. W.; Lu, Y. J. *J. Am. Chem. Soc.* **2004**, *126*, 12298–12305.
(17) Liu, J. W.; Lu, Y. *Anal. Chem.* **2004**, *76*, 1627–1632.
(18) Wang, Z. D.; Lee, J. H.; Lu, Y. *Adv. Mater.* **2008**, *20*, 3263–3267.
(19) Wang, Z. D.; Lu, Y. *J. Mater. Chem.* **2009**, *19*, 1788–1798.
(20) Wei, H.; Li, B. L.; Dong, S. J.; Wang, E. K. *Nanotechnology* **2008**, *19*, 095501.
(21) Ali, E. M.; Zheng, Y. G.; Yu, H. H.; Ying, J. Y. *Anal. Chem.* **2007**, *79*, 9452–9458.
(22) Wu, Q. Z.; Cao, H. Q.; Luan, Q. Y.; Zhang, J. Y.; Wang, Z.; Warner, J. H.; Watt, A. A. R. *Inorg. Chem.* **2008**, *47*, 5882–5888.
(23) Briñas, R. P.; Hu, M. H.; Qian, L. P.; Lymar, E. S.; Hainfeld, J. F. *J. Am. Chem. Soc.* **2008**, *130*, 975–982.
(24) Liu, X.; Dai, Q.; Austin, L.; Coutts, J.; Knowles, G.; Zou, J. H.; Chen, H.; Huo, Q. *J. Am. Chem. Soc.* **2008**, *130*, 2780–2782.
(25) He, S. J.; Li, D.; Zhu, C. F.; Song, S. P.; Wang, L. H.; Long, Y. T.; Fan, C. H. *Chem. Commun.* **2008**, 4885–4887.
(26) Huang, K. W.; Yu, C. J.; Tseng, W. L. *Biosens. Bioelectron.* **2010**, *25*, 984–989.
(27) Wang, Y.; Yang, F.; Yang, X. R. *ACS Appl. Mater. Interfaces* **2010**, *2*, 339–342.
(28) Kim, Y. R.; Mahajan, R. K.; Kim, J. S.; Kim, H. *ACS Appl. Mater. Interfaces* **2010**, *2*, 292–295.
(29) Huang, C. C.; Chang, H. T. *Anal. Chem.* **2006**, *78*, 8332–8338.
(30) Darbha, G. K.; Ray, A.; Ray, P. C. *Acs. Nano.* **2007**, *1*, 208–214.
(31) Chiang, C. K.; Huang, C. C.; Liu, C. W.; Chang, H. T. *Anal. Chem.* **2008**, *80*, 3716–3721.
(32) Liu, C. W.; Huang, C. C.; Chang, H. T. *Anal. Chem.* **2009**, *81*, 2383–2387.
(33) Li, T.; Dong, S. J.; Wang, E. K. *Anal. Chem.* **2009**, *81*, 2144–2149.

AM100107K